Original Article

Institution of MECHANICAL ENGINEERS
Journal of MECHANICAL ENGINEERING SCIENCE

Proc IMechE Part C:
J Mechanical Engineering Science
2015, Vol. 229(18) 3459–3472

DOI: 10.1177/0954406215570106
pic.sagepub.com
SAGE

Design and optimization of a new kind of hydraulic cylinder for mobile robots

Yong Xue, JunHong Yang, JianZhong Shang and HuiXiang Xie

Abstract

In order to improve the efficiency of multi-actuator mobile robots hydraulic system, this paper proposes a new kind of cylinder whose effective area is variable. The new cylinder has multi chambers which can be connected with each other or to a main system circuit by controlling switching valves. On the one hand, the new cylinder can make sure that the load pressure of all actuators is almost equal through varying effective area. On the other hand, the new cylinder can realize the flow recovery through that return chambers are connected with feeding chambers. Therefore, the new cylinder can reduce overall machine energy consumption by reducing throttling losses and allowing energy recovery. The performance of the new cylinder is analyzed through building the mathematical model. Based on the evaluated results, in order to further improve the performance of the load match of the cylinder and avoid the deflection of the main piston, the structure of the cylinder is optimized. Finally, an optimized cylinder is shown in this paper which has well performance of the load match.

Keywords

Hydraulic cylinder, high efficiency, variable effective area, mobile robot

Date received: 27 July 2014; accepted: 30 December 2014

Introduction

At present, the hydraulic system used in legged robot has become a main studying interest for improving the load capacities and endurance of legged robots,[1] such as the famous Bigdog and Petman robots developed by Boston Dynamics Company,[2–4] LS3, Chetah and HyQ.[5] Durfee et al.[6] have proposed that hydraulic drives have higher power density than electromechanical drives when the pressure of power source is larger than 3.5 MPa. However, the efficiency of fluid power systems is generally low versus the mechanical or electric transmission system.[7]

From the existing research on legged robot hydraulic systems,[2–5,8,9] researchers usually utilize a single pump source and multi-actuators structure to minimize the weight of the robot. The efficiency of a hydraulic system with a single power source and multiple actuators is very low when the load change of actuators is different. Total cost of transport (COT) is widely used to measure the efficiency of legged animals and robots, is given by the power consumption divided by the weight times velocity.[10] Compared to animals, the COT of legged robots such as ASIMO (COT = 2) and Boston Dynamics BigDog (COT = 15) is significantly higher than animals with similar masses.[11,12] The low efficiency of the hydraulic system is a main factor which causes the high total COT for the Bigdog. In Zoss et al.,[13] the power curve of each joint is described as a person (75 kg) is walking on the flat ground at a speed of 1.3 m/s. The change of each joint power curve is very obvious, and the efficiency of the hydraulic system for lower extremity exoskeleton is only 14%. The reason for this is each actuator of a legged robot has a different load at the same time, and any one actuator has widely fluctuating load forces and displacements over time. However, the system pressure only can match one actuator's load, usually the largest load at one moment, so a lot of throttling losses are produced. Low efficiency will lead to larger power required and more heating which will need a larger cooling system. Then larger power will lead to bigger and heavier power sources. In addition, environmental issues and rising oil prices, along with ever tighter legislation on emissions also stimulate the development of more energy-efficient hydraulic systems.[7]

There have been a few approaches to improve the efficiency of hydraulic systems for mobile robots.

College of Mechatronic Engineering and Automation, National University of Defense Technology, Changsha, China

Corresponding author:
JunHong Yang, Department of Mechatronic Engineering and Automation, National University of Defense Technology, Changsha 410073, China.
Email: yangjunhong@nudt.edu.cn

For example, The DC–DC switching Buck converter has been used to improve the efficiency of the hydraulic system.[14–16] In order to make every branch's pressure match with the load, a DC–DC switching Buck converter before every cylinder needs to be applied, whose weight is 14 kg in the literature.[15] Alfayad et al.[17] have proposed a hydrostatic transmission actuator which is controlled by displacement and has capacities for energy storage. But preliminary experimental results presented the capacity of this prototype, moving approximately 38 kg at 2 cm/s.

At present, researchers have been proposed many approaches to improve the hydraulic systems efficiency of multi-actuator machines. Dr Monika Ivantysynova' research group has extensively studied a promising technology of displacement controlled (DC) actuation since a first promising solution for linear actuators with single rod cylinders.[18–20] Payne et al.[21] have proposed the digital pump-motor technology that is claimed to significantly improve the energy efficiency of hydraulic systems but has multiple independent outlets. Shen et al.[22] have proposed one new-type hydraulic transformer which is composed of two main parts that are a swash plate-type pump and a part is similar to a swing vane motor.[22] In addition, there are other methods, such as electric-hydraulic hybrid energy recovery methods,[23] load sensitive technology,[24] double-pump or multi-pump matching different load force of actuators, technology of independent metering valve ports,[25,26] etc. To a certain extent, these methods could improve the efficiency of the multi-actuator hydraulic system. However, these methods are not good choice for improving legged robot hydraulic system efficiency since the legged robot requires high dynamic characteristics, light weight and small size. Hence, it is necessary to develop new methods with high efficiency to promote the practical use of legged robots forward.

Due to the main factor that causes the low efficiency of the multi-actuator mobile robots hydraulic system is that the output forces of actuators do not match the load, the paper proposes a new kind of cylinder whose effective area can be adjusted to make sure that the load pressure of all the actuators is almost equal. The hydraulic power source of mobile robots usually adopts a constant pressure variable pump which can keep its flow automatically varying to match the total load flow. Therefore, the efficiency of the hydraulic system which is composed of a constant pressure variable pump and the new cylinders is very high. The new cylinder can be applied in the mobile robots whose actuators usually have widely fluctuating load forces. For example, Figure 1 shows that the new cylinder is used to drive the forearm of a human robot.

The organization of this paper is as follows. In the next section, the principle of varying effective area and the structure of the new cylinder is presented. Then the performance of load match of the new cylinder is presented followed by the section that presents the performance of the structure of the new cylinder. Next, the optimization design of the new cylinder is presented followed by the section that shows the performance of the load match and the structure of the optimized cylinder. Finally, conclusions are presented.

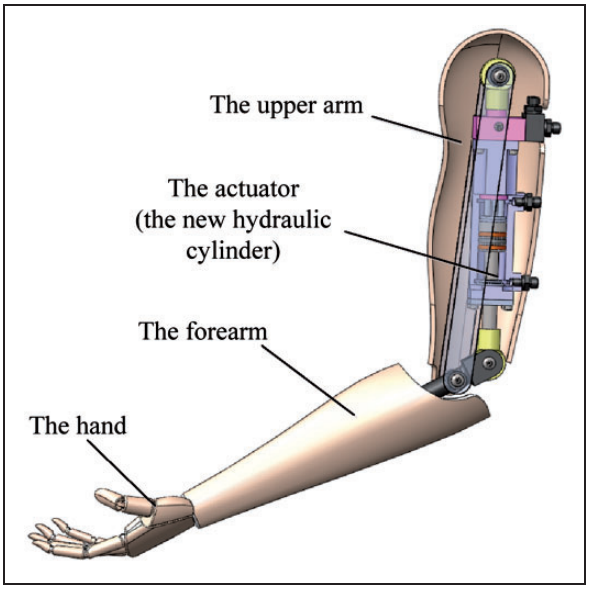

Figure 1. The forearm of a human robot driven by the new cylinder.

Design of the cylinder with varying effective area

In this section, the mechanism of the new cylinder with varying effective area is presented, and then the structure of the cylinder is designed.

Principle of varying effective area for the new cylinder

The principle of the cylinder with variable effective area is in the dashed box shown in Figure 2. It is composed of four 3/2 switching valves and one cylinder with multi chambers and multi piston rods. The plunger chambers A_1, A_2, A_3 and A_4 can be connected with the left chamber A_l or the right chamber A_r through controlling the 3/2 switching valves P_1, P_2, P_3 and P_4. Different control of the four switching valves corresponds to different connections and means different effective area. For example, when the main rod extends, if the plunger chamber A_1 connects with the left chamber A_l and other plunger chambers connect with the right chamber A_r, the effective areas are A_1 and A_l. The oil which flows in the chambers A_1 and A_l is supplied by the power source, but which flows in the chambers A_2, A_3 and A_4 comes from the right chamber A_r. If the volume of oil which flows in the chambers A_2, A_3 and A_4 is more than that of oil which flows out the right chamber A_r,

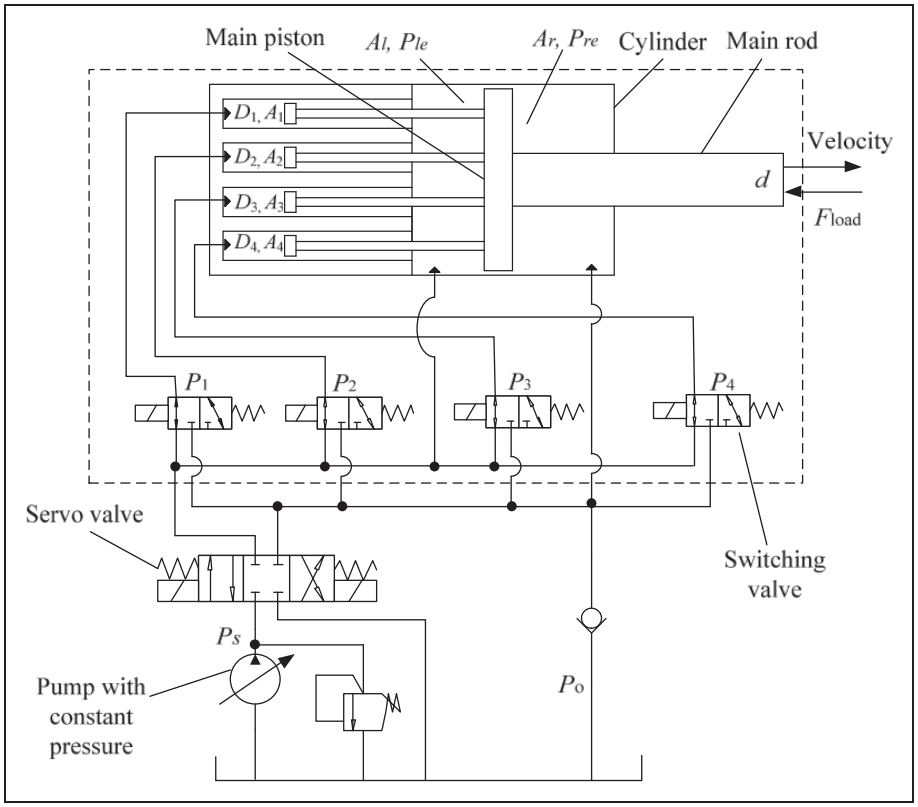

Figure 2. The principle of the cylinder with varying effective area.

the shortage of oil can be supplied by the oil trunk through the port T of servo valve or the non-returning valve. When the main rod retracts, if the plunger chamber A_1 connects with the right chamber A_r and other plunger chambers connect with the left chamber A_l, the effective area is the difference area of the chamber A_1 and chamber A_r. The oil which flows in the right chamber A_r is not all supplied by the power source, but a part of oil comes from chamber A_1.

The effective area of the new cylinder can be adjusted through controlling the switching valves P_1, P_2, P_3 and P_4 to make sure that the maximal putout force is close to the load force, so the system can keep constant pressure. For the ordinary hydraulic cylinder whose effective area is fixed, when the load force is decreased but the velocity of the rod is unaltered, it needs to reduce the input pressure to match the load force by increasing the metering loss of the servo valve. More metering loss leads to lower efficiency. However, the new cylinder does not need to reduce the input pressure to match the load force through decreasing the effective area. Of cause, the adjustment of the effective area is discrete, so the maximal output force of the new hydraulic cylinder may be a little higher than the load force. For keeping the changeless velocity of the rod, it only needs to adjust a little the open of the servo valve. In addition, because a part of oil which flows out the right chamber A_r flows in some plunger chambers, the metering loss of the servo valve's port T is decreased obviously. Less metering loss leads to higher efficiency of the hydraulic system.

In summary, on the one hand, the new cylinder can make sure that the load pressure of all actuators is almost equal through varying effective area. On the other hand, the new cylinder can realize the flow recovery through that return chambers are connected with feeding chambers. Therefore, the new cylinder can reduce overall machine energy consumption and improve the efficiency of the hydraulic system by reducing throttling losses and allowing energy recovery. The new cylinder not only remains the high performance properties of valve-control but also reduces the energy losses.

Structure design of the new cylinder

In "Principle of varying effective area for the new cylinder" section, the principle of the new cylinder has been presented. When the new cylinder is designed, the number of the plunger chambers is determined according to the practical load force. Of course, more number of the plunger chambers means more ratings of the effective area of the new cylinder and higher efficiency of the hydraulic system, but the manufacture difficulties increase. In this paper, as shown in Figure 3, the new cylinder has four plunger chambers A_1, A_2, A_3 and A_4. In order to obtain most ratings of the effective area, namely, $C_4^0 + C_4^1 + C_4^2 + C_4^3 + C_4^4$, the cross sectional area of the plunger chamber A_1 is S, and then the cross sectional areas of the chambers A_2, A_3 and A_4 are set as two times S, four times S and 8 times S, respectively.

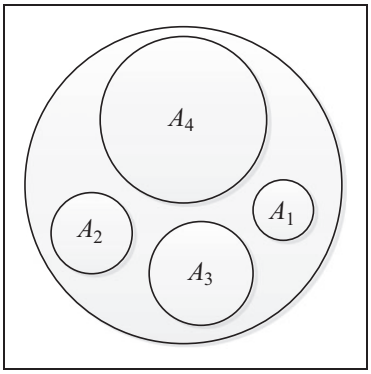

Figure 3. The structure of the multi chambers.

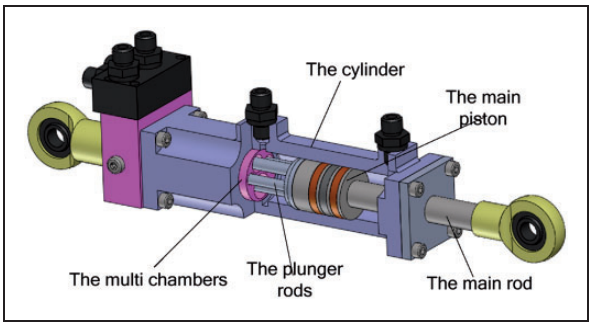

Figure 4. The structure of the cylinder with variable effective area.

Therefore, there are 16 different effective areas, namely, 0S, 1S, 2S, 3S, 4S, 5S, 6S, 7S, 8S, 9S, 10S, 11S, 12S, 13S, 14S and 15S.

The structure of the cylinder with variable effective area is shown in Figure 4, which is mainly composed of the cylinder, the main piston, the main rod, the multi chambers and the plunger rods which are fixed to the main piston. The new cylinder has six oil ports which are connected with the chambers A_1, A_2, A_3, A_4, A_l and A_r, respectively.

In order to evaluate the performance of the cylinder's load match, the mathematics model of the new cylinder is established in ''Performance of the load match for the new cylinder'' section.

Performance of the load match for the new cylinder

For the new cylinder, it is critical to determine the effective areas and the distribution of the cylinder's output force for different settings of the switching valves.

Mathematics model of the new cylinder

Defining the control of the four switching valves by $x=[x_1\ x_2\ x_3\ x_4]$, where $x_k=1$ $(k=1\text{–}4)$ means that chamber A_k is connected to the left chamber A_l, and $x_k=0$ means that chamber A_k is connected to the right chamber A_r. S_k is the piston's area of chamber A_k, and S_L is the cross sectional area of left chamber A_l which is the area of main piston excluding the area S_1, S_2, S_3 and S_4. S_r is the cross sectional area of right chamber A_r which is the area of main piston excluding the area of the main rod. Therefore, the relationship between the left effective area S_{le}, the right effective area S_{re} and switching valve-control x can be expressed as follows

$$S_{le} = S_L + \sum_{k=1}^{4} S_k x_k \tag{1}$$

$$S_{re} = S_r + \sum_{k=1}^{4} S_k (x_k - 1) \tag{2}$$

Neglecting the throttling pressure loss of the switching valve, the output force of the cylinder F_{op} is as follows

$$F_{op} = P_{le} S_{le} - P_{re} S_{re} \tag{3}$$

where P_{le} and P_{re} are the pressures of the left chamber and the right chamber of the main piston, respectively.

From equations (1) to (3), the output force of the cylinder F_{op} can be expressed as follows

$$F_{op} = P_{le} S_L - P_{re}(S_r - \sum_{k=1}^{4} S_k) + (P_{le} - P_{re}) \sum_{k=1}^{4} S_k x_k \tag{4}$$

Equation (4) indicates that the controllable change of $\sum_{k=1}^{4} S_k x_k$ determines the change of the cylinder's output force.

On the assumption that the oil is rigid, the flows into or out of the chambers are obtained

$$Q_l = v S_{le} \tag{5}$$

$$Q_r = v S_{re} \tag{6}$$

where Q_l is the flow rate which flows into or out of the chambers whose area is S_{le}, and Q_l is defined as positive when oil flows into the cylinder. Q_r is the flow rate which flows into or out of the chambers whose area is S_{re}, and Q_r is defined as positive when oil flows into the oil tank from the cylinder. v is the velocity of main piston rod, and it is defined as positive when the piston rod moves to the right.

In addition, w, C_d, ρ and u are defined as the valve opening gradient, the flow coefficient, the density of oil and the servo valve-control signal, respectively. According to Bernoulli's orifice equation and

neglecting valve dynamics, when $u > 0$, $v > 0$, the flows Q_l and Q_r are expressed as follows

$$Q_l = C_d w u \sqrt{\frac{2}{\rho}(P_s - P_{le})} \quad (Q_l > 0) \tag{7}$$

$$Q_r = C_d w u \sqrt{\frac{2}{\rho}(P_{re} - P_o)} \quad (S_{re} > 0,\ Q_r > 0) \tag{8}$$

$$Q_r = -C_d w u \sqrt{\frac{2}{\rho}(P_o - P_{re})} \quad (S_{re} < 0,\ Q_r < 0) \tag{9}$$

When $u < 0$, $v < 0$, the flows Q_l and Q_r are expressed as follows

$$Q_l = C_d w u \sqrt{\frac{2}{\rho}(P_{le} - P_o)} \quad (Q_l < 0) \tag{10}$$

$$Q_r = C_d w u \sqrt{\frac{2}{\rho}(P_s - P_{re})} \quad (Q_r < 0) \tag{11}$$

When $u < 0$, $v > 0$ ($\sum_{k=1}^{4} S_k > S_r$), the flows Q_l and Q_r

are expressed as follows

$$Q_l = -C_d w u \sqrt{\frac{2}{\rho}(P_o - P_{le})} \quad (Q_l > 0) \tag{12}$$

$$Q_r = C_d w u \sqrt{\frac{2}{\rho}(P_s - P_{re})} \quad (Q_r < 0) \tag{13}$$

Synthesizing equations (8) to (14), the unified pressure-flow equations can be obtained

$$Q_l = \mathrm{sgn}(\Delta P_{le}) C_d w u \sqrt{\frac{2}{\rho}|\Delta P_{le}|} \tag{14}$$

$$Q_r = \mathrm{sgn}(\Delta P_{re}) C_d w u \sqrt{\frac{2}{\rho}|\Delta P_{re}|} \tag{15}$$

$$\Delta P_{le} = (1+\mathrm{sgn}(u))P_s/2 + (\mathrm{sgn}(u)-1)P_o/2 - \mathrm{sgn}(u)P_{le} \tag{16}$$

$$\Delta P_{re} = (1-\mathrm{sgn}(u))P_s/2 - (\mathrm{sgn}(u)+1)P_o/2 + \mathrm{sgn}(u)P_{re} \tag{17}$$

From equations (5), (6), (14) and (15), the pressures P_{le} and P_{re} can be obtained

$$P_{le} = P_s(1 + \mathrm{sgn}(u))/2 + P_o(1 - \mathrm{sgn}(u))/2 - 0.5\rho \cdot \mathrm{sgn}(Q_l) \cdot \left(\frac{Q_l}{C_d w u}\right)^2 \tag{18}$$

$$P_{re} = P_s(1 - \mathrm{sgn}(u))/2 + P_o(1 + \mathrm{sgn}(u))/2 + 0.5\rho \cdot \mathrm{sgn}(Q_r) \cdot \left(\frac{Q_r}{C_d w u}\right)^2 \tag{19}$$

Output force of the new cylinder

The MATLAB Simulation tool is used for the simulations of the output force of the new hydraulic cylinder. The simulation parameters of the hydraulic system are shown in Table 1.

According to the design principle of the multi chambers' area and the structure of the new hydraulic cylinder which have been presented in "Structure design of the new cylinder" section, the diameter of the chamber A_1 is set as 5 mm, which can ensure that the four plunger chambers are designed on the main piston. Then the diameter of the chambers A_2, A_3 and A_4 is set as 7 mm, 10 mm and 14 mm, respectively.

When the opening of the servo valve keeps positive maximum value, there are 16 different area values of $\sum_{k=1}^{4} S_k x_k$ corresponding to 16 different rating $x = [x_1\ x_2\ x_3\ x_4]$, for example, [0 0 0 0] is the first rating, [1 0 0 0] is the second rating, [0 1 0 0] is the third rating and [1 1 1 1] is the sixteenth rating. Different area value means different output force and 16 different rating output forces of the new cylinder can match 16 different pressure loads. When the opening of the servo valve keeps negative maximum value, in the same way 16 different rating output forces of the new cylinder can match 16 different pulling loads. The different output forces of the new cylinder are shown in Figure 5.

As shown in Figure 5, there is a big jump when the control signal of the servo valve passes through zero. Therefore, the load matching cannot be realized when the change of the load is between −5030 N and 6560 N. To reduce the size of the jump, it is necessary

Table 1. Simulation parameters of the hydraulic system.

Parameter	Value
Opening of servo valve (mm)	−1 to 1
Spool circumference of servo valve (mm)	6.28
Pressure of tank (MPa)	0.1
Opening area of switching valve (mm^2)	25.1
Coefficient of flow for switching valve	0.6
Coefficient of flow for servo valve	0.67
Density of oil (kg/m^3)	875
Pressure of power source (MPa)	16
On-off value of four switching valves	0 or 1
Velocity of piston rod (mm/s)	200
Diameter of main Piston (mm)	30
Diameter of main Rod (mm)	15

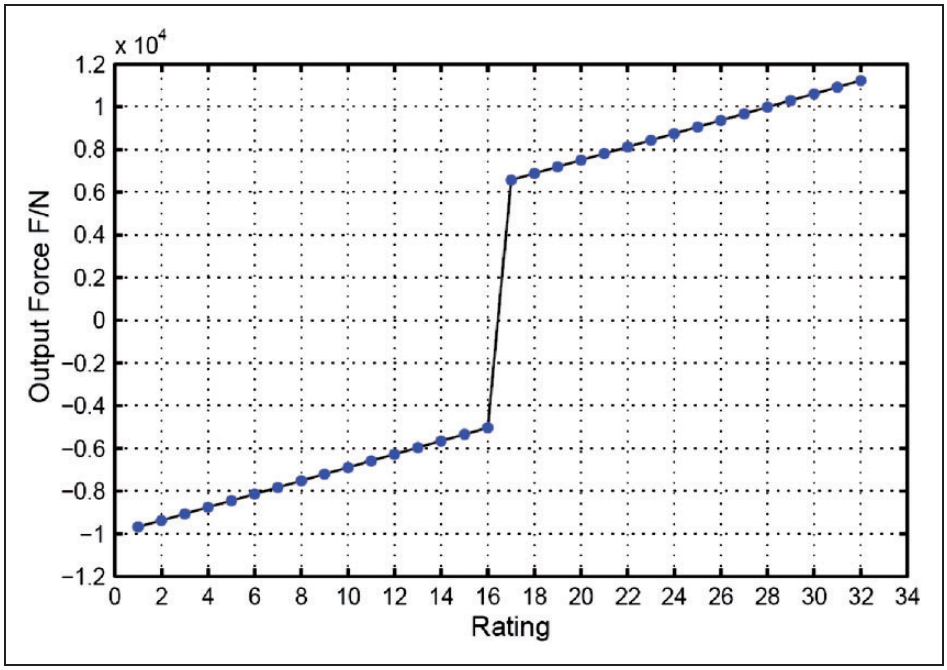

Figure 5. The output force of the new cylinder in the different rating. The positive value is the pressure loads corresponding to the extending of the cylinder. The negative value is the pulling loads corresponding to the retracting of the cylinder. The dot corresponding to the force is the maximal value in a rating.

to reduce the value of S_l and adjust the four plunger chambers' area.

Performance of the structure of the new cylinder

According to the structure of the new cylinder, the chambers cannot be distributed symmetrically due to the areas of chambers A_1, A_2, A_3 and A_4 are not equal, and the action force of every plunger rod does not pass the center of the main piston, so the composition of the forces of plunger rods may lead to the deflection of main piston. However, the deflection can cause the inner leak of the cylinder. Therefore, it is necessary to analyze the deflection of the main piston and optimize the structure.

Deflection of the main piston

As shown in Figure 6, the Cartesian coordinate system Oxy is located in the centre of the piston. O, O_1 are the center of the main piston and rod end, respectively. F_1, F_2, F_3 and F_4 are the action forces of the plunger rods, and K_1, K_2, K_3 and K_4 are the center of the action forces, respectively. α, β and γ are the acute angles between the y axis and the beeline OK_1, OK_2 and OK_3, respectively. r is the diameter of the main rod.

For convenient calculation, F_1, F_2, F_3 and F_4 are simplified to the torque of the couples and the forces whose load position is the point O, and then the torque of the couple is divided into the

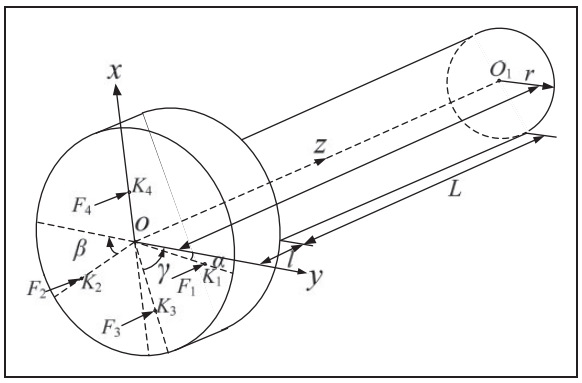

Figure 6. The mathematical model of the main piston.

bending moments M_x and M_y which are in the principle inertia plane Oyz and Oxz, respectively. Due to the forces whose load position is the point O cannot lead to the bend of the main rod, it only need to analyze the bends which are caused by the bending moment M_x and M_y. Defining R_1, R_2, R_3 and R_4 are the distances from the point O to the points K_1, K_2, K_3 and K_4, respectively and L is the stroke of the new cylinder. Defining the direction of the force in Figure 8 is the positive, the M_x and M_y can separately be obtained

$$M_x = F_1 R_1 \cos\alpha + F_3 R_3 \cos\gamma - F_2 R_2 \cos\beta \quad (20)$$

$$M_y = F_4 R_4 - F_1 R_1 \sin\alpha - F_2 R_2 \sin\beta - F_3 R_3 \sin\gamma \quad (21)$$

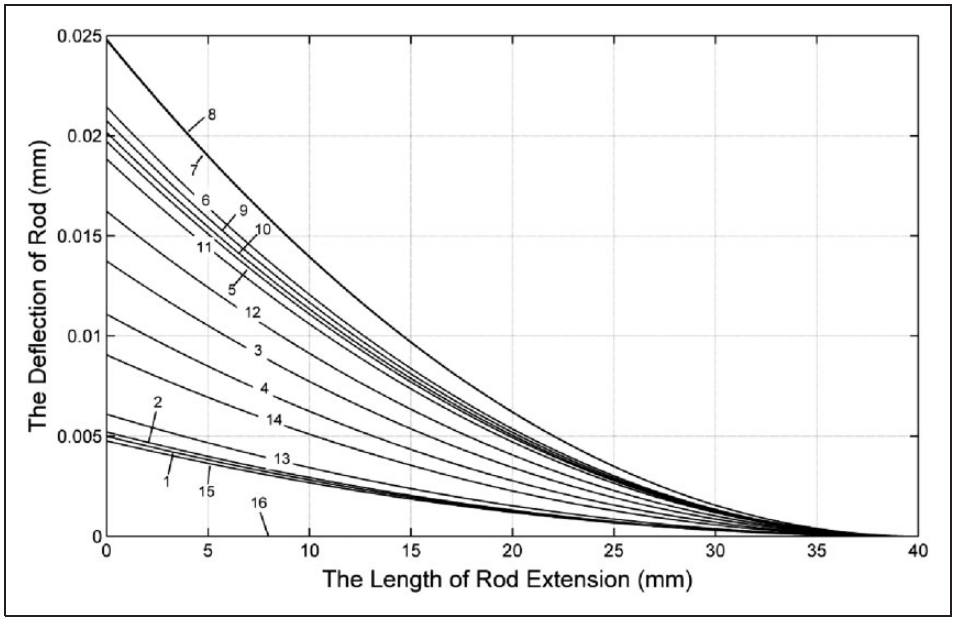

Figure 7. The total deflection of the main rod at the different rating. The process is the retracting of the cylinder, and the numerals in the line denote the ratings of the varying effective area.

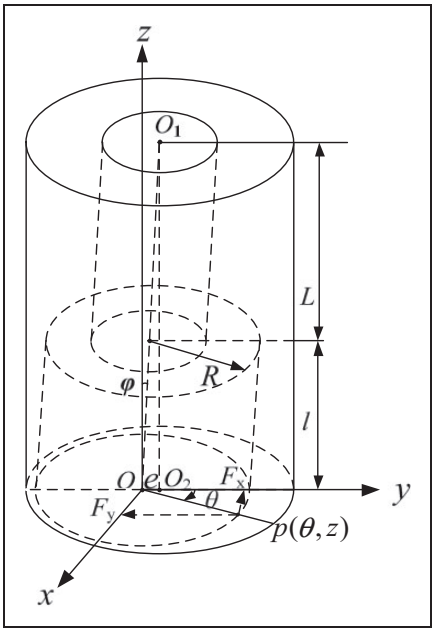

Figure 8. The deflection model of the main piston.

Therefore, the deflections w_1 and w_2 which are caused by the bending moments M_x and M_y are obtained

$$w_1 = \frac{M_x(L-z)^2}{2EI_x} \tag{22}$$

$$w_2 = \frac{M_y(L-z)^2}{2EI_y} \tag{23}$$

where E is the material elastic modulus of the main rod, I_x, I_y is the moment of inertia and $I_x = I_y = I$.

Because the diameter of the main piston is much larger than the diameter of the main rod, by neglecting the bend of the piston, the total deflection w and the main rod' rotation angle φ is obtained

$$w = \sqrt{w_1^2 + w_2^2} = \frac{\sqrt{M_x^2 + M_y^2}}{2EI}(L-z)^2 \tag{24}$$

$$\varphi = \sqrt{w_1^2 + w_2^2} = \frac{\sqrt{M_x^2 + M_y^2}}{EI}(L-z) \tag{25}$$

In addition, the forces F_1, F_2, F_3 and F_4 can be derived

$$F_{k=1,\,2,\,3,4} = (P_{le} - P_{re})(x_k - 1)A_k \tag{26}$$

where the pressures P_{le} and P_{re} can be obtained by equations (18) and (19), respectively.

Therefore, the deflection w of the main rod can be obtained by MATLAB. The simulation parameters of the hydraulic system have been shown in Table 1 and other calculation parameters are shown in Table 2.

Figure 7 shows the deflection changes of the main rod at the different rating when the rod of the cylinder retracts. As shown in Figure 7, the stroke of the cylinder is longer, the deflection of the piston is more remarkable. For all ratings, the most deflections of the main piston all appear at the time of the rod retracting totally and the most deflection that is 0.0248 mm appears at the eighth rating, namely, the $x = [1\ 1\ 1\ 0]$, in other words, the chambers A_1, A_2 and A_3 are connected with the chamber A_l, but the chamber A_4 is connected with the chamber A_r. However, the deflection at the 16th rating is zero, due to all the chambers A_1, A_2, A_3 and A_4 are connected with the

Table 2. Summary of parametric data used for calculating the deflection of the main rod.

Parameters	Value
Distance from the point O to K_1 (mm)	10
Distance from the point O to K_2 (mm)	9.5
Distance from the point O to K_3 (mm)	8.5
Distance from the point O to K_l (mm)	6.5
Stroke of the cylinder (mm)	40
Length of the main piston (mm)	30
Acute angle between the y axis and the beeline OK_1 (rad)	0.11
Acute angle between the y axis and the beeline OK_2 (rad)	0.56
Acute angle between the y axis and the beeline OK_3 (rad)	1.22
Inertia moment of the main rod (mm^4)	2485
Material elastic modulus (Gpa)	210

chamber A_l, namely, the forces F_1, F_2, F_3 and F_4 are zero.

In addition, according to equation (26), when the rod of the cylinder extends, the directions of the forces F_1, F_2, F_3 and F_4 are inverse but whose value are almost equal relative to that the rod of the cylinder retracts, so the characteristic of the deflections are almost same compared to which is shown in Figure 7.

However, because more deflection can lead to more leakage and abrasion of the piston, the leak of the new cylinder is analyzed in the next section.

Leakage of the new cylinder

The main piston of the hydraulic cylinder usually adopts the contact mechanical seal. For this seal, there is thin oil film between the face of the seal ring and the inner wall of the cylinder. Commonly, the thickness of the oil film is only 0.5 μm to 2 μm.[27] However, based on the discussion of the new cylinder in the above section, in practical working, the center of the main piston may occur to the deflection which leads to that the gap increases at one side of the main piston and the seal ring is compressed at other side. Therefore, the abrasion of the seal ring is accelerated and the inner leakage of the cylinder increases.

In order to analyze the inner leak of the cylinder after the sealing failure of the main piston' seal ring, the mathematic model about the deflection of the main piston is established in Figure 8. The Cartesian coordinate system Oxy is located in the centre of the main piston, and the most deflection of the main piston is located on the y axis. R is the diameter of the main piston. e is the most deflection of the main piston. φ the main rod' rotation angle, p is the oil film's pressure.

On the assumption that the oil is rigid, for the deflection model of the main piston, the Reynolds equation is

$$\frac{1}{R^2}\frac{\partial}{\partial\theta}\left(\frac{h^3}{\mu}\frac{\partial p}{\partial\theta}\right)+\frac{\partial}{\partial z}\left(\frac{h^3}{\mu}\frac{\partial p}{\partial z}\right)=6v\frac{\partial h}{\partial z} \tag{27}$$

where h is the thickness of the oil film, μ is the dynamic viscosity, v is the velocity of the piston.

The thickness of the oil film is not a fixed value due to the deflection of the main piston. Defining that δ is the gap between the piston and inner wall of the cylinder when the main piston does not deflect, the thickness of the oil film h is obtained

$$h=\delta+[(l-z)\tan\varphi+w]\cos\theta \tag{28}$$

where the deflection w and the main rod's rotation angle φ are calculated by equations (24) and (25), respectively.

If let

$$z=Z\cdot l$$
$$h=\delta\left(1+\frac{(1-Z)l\sin\varphi+w}{\delta}\cos\theta\right)=\delta H$$
$$p=P\frac{6U\mu R^2}{l\delta^2}$$
$$a=(R/l)^2$$

The normalization of equation (27) is obtained

$$A\frac{\partial^2 P}{\partial\theta^2}+B\frac{\partial^2 P}{\partial z^2}+C\frac{\partial P}{\partial\theta}+D\frac{\partial P}{\partial Z}=E \tag{29}$$

where the coefficients are

$$A=1$$
$$B=(R/l)^2$$
$$C=-\frac{3\sin\theta}{\delta H}[(1-z)l\sin\varphi+w]$$
$$D=-\frac{3R^2\sin\varphi\cos\theta}{\delta l H}$$
$$E=-\frac{l\sin\varphi\cos\theta}{\delta H^3}$$

The relationships between every nodal point's oil film pressure $P_{i,j}$ and the adjacent nodal points' oil film pressures can be obtained through the finite difference method, namely

$$P_{i,j}=C_N P_{i,j+1}+C_S P_{i,j-1}+C_E P_{i+1,j}+C_w P_{i-1,j}+G \tag{30}$$

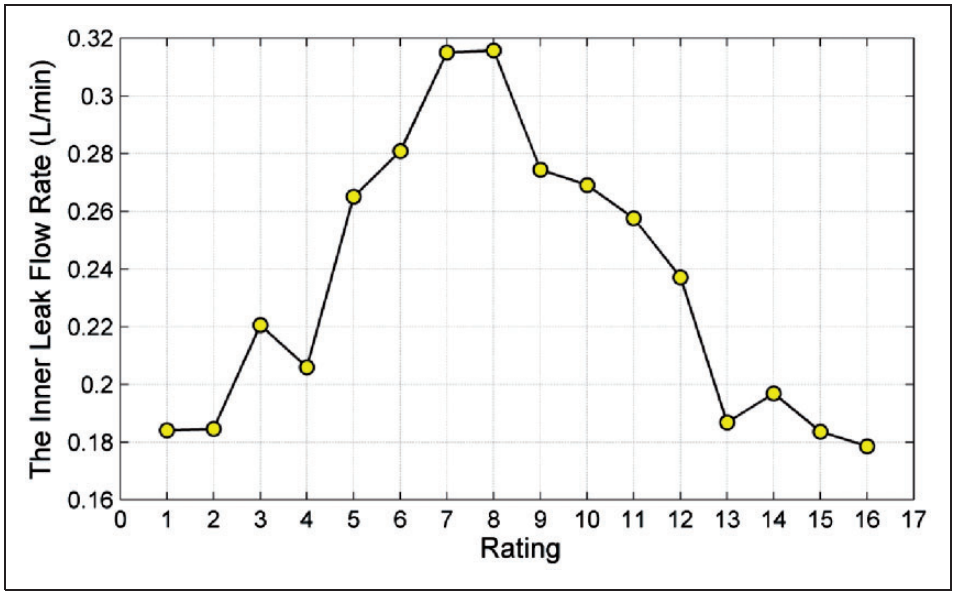

Figure 9. The inner leak flow rate of the new cylinder at the different rating. The yellow dot corresponding to the flow rate is the maximal value in a rating.

where the coefficients are

$$C_N = \left(\frac{B}{\Delta z^2} + \frac{D}{2\Delta z}\right)/K$$
$$C_s = \left(\frac{B}{\Delta z^2} - \frac{D}{2\Delta z}\right)/K$$
$$C_E = \left(\frac{A}{\Delta \theta^2} + \frac{C}{2\Delta \theta}\right)/K$$
$$C_w = \left(\frac{A}{\Delta \theta^2} - \frac{C}{2\Delta \theta}\right)/K$$
$$G = -\frac{E}{K}$$
$$K = 2\left(\frac{A}{\Delta \theta^2} + \frac{B}{\Delta z^2}\right)$$

The boundary condition is (1) $Z=0$, $P=\frac{P_{le}l\delta^2}{6v\mu R^2}$; (2) $Z=1$, $P=\frac{P_{re}l\delta^2}{6v\mu R^2}$; (3) $\theta=0$ or $\theta=\pi$, $\frac{\partial P}{\partial \theta}=0$. The pressures P_{le} and P_{re} can be calculated through equations (18) and (19), respectively.

The condition of iterative convergence is

$$\frac{\sum\sum|P_{i,j}^{k+1}-P_{i,j}^{k}|}{\sum\sum P_{i,j}^{k+1}} \leqslant \varepsilon \tag{31}$$

where ε is the relative precision, generally is 0.01–10^{-6}.

Therefore, using the condition of the iterative convergence and the boundary condition, the numerical solution of oil film pressure can be worked out through the iterative calculation of equation (30), and then the inner leakage flow rate of the new cylinder is obtained

$$\bar{Q} = \frac{Q}{U\delta R} = \int_0^{2\pi}\left(\frac{H}{2} - a\frac{H^3}{2}\frac{\partial P}{\partial Z}\right)\mathrm{d}\theta = \int_0^{2\pi} q\mathrm{d}\theta \tag{32}$$

Table 3. Summary of parametric data used for calculating the leakage.

Parameter	Value
Velocity of piston rod (mm/s)	200
Gap between piston and inner wall (mm)	0.03
Dynamic viscosity (Pa · s)	0.042
Diameter of the main piston (mm)	15
Relative precision	10^{-4}

where Q is the inner leakage flow rate, $\bar{Q}$ is the dimensionless variable.

Equation (32) can be worked out through the method of the numerical integration based on the Simpson's theorem.

$$\bar{Q} = \frac{2\pi}{3(n-1)}(q_1 + 4q_2 + 2q_3 + 4q_4 + \cdots + q_n) \tag{33}$$

where n is the number of the node point, $q_1, q_2, \ldots, q_n$ are the flow rates corresponding to the node points.

Therefore, the inner leakage flow rate of the new cylinder Q can be calculated by MATLAB, as shown in Figure 9. The simulation parameters have been shown in Table 3.

As shown in Figure 9, for the different rating, the inner leak flow rate of the new cylinder is different and the most leakage appears at the eighth rating due to the most deflection. The most leak flow rate reaches 0.316 L/min which is the 1.77 times the least leak flow rate that appears at the 16th rating.

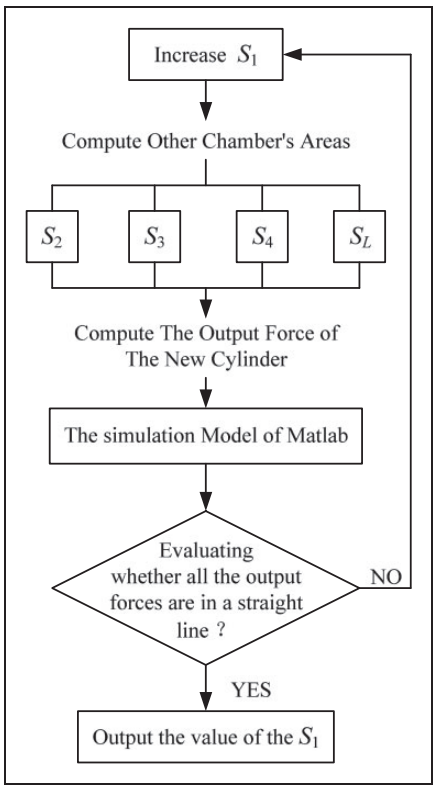

Figure 10. The optimization method of the variable effective areas.

However, due to the leakage of the new cylinder will reduce the efficiency of the hydraulic system, in order to make the efficiency higher, it is necessary to optimize the structure of the multi chambers to avoid the deflection of the main piston.

Optimization design of the new cylinder

In order to improve performance of the load matching of the new cylinder and to avoid the deflection, it is necessary to optimize the variable effective areas and the structure of the new hydraulic cylinder.

Optimization of the variable effective area

The optimization method for the variable effective area of the new cylinder is illustrated in Figure 10. The first step is to increase the area of the chamber A_1 based on the diameter 5 mm, and then to compute the other chambers' area according to the design principle which has been presented in "Structure design of the new cylinder" section. The second step is to work out all the output force of the new cylinder by the mathematic model which has been detailed in Mathematics model of the new cylinder section. The next step is to evaluate whether all the output forces are in a straight line. If the evaluation result does not satisfy the demand, the procedure returns to the first

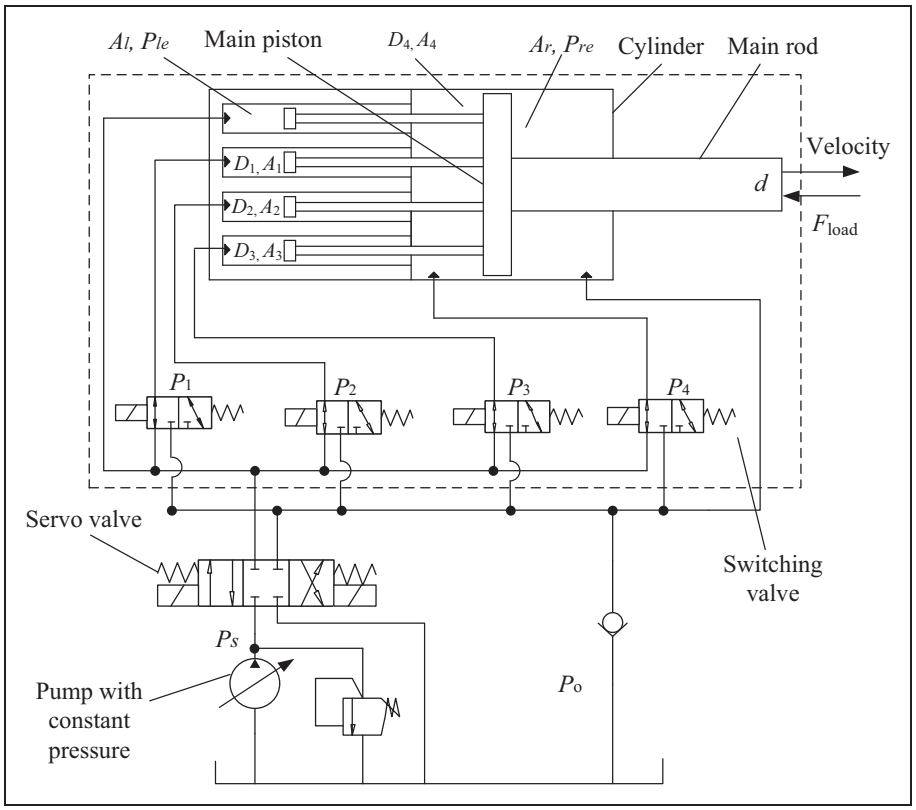

Figure 11. The new structure of the cylinder with variable effective area.

step automatically and computes again. The last step is to output the satisfy area value of the chamber A_1.

An optimization diameter of the chamber A_1 is chosen by the above method. The optimization diameters of the chambers A_1, A_2, A_3 and A_4 are 7.4 mm, 10.5 mm, 14.8 mm and 20.9 mm, respectively. However, due to the diameter of the main piston is only 30 mm, all the chambers A_1, A_2, A_3 and A_4 cannot be distributed together. Therefore, it is necessary to adjust the structure of the cylinder. According to the principle of the new cylinder which has shown in Figure 2, the places of the chamber A_4 and chamber A_l can be exchanged due to the area of the chamber A_l is only 62.2 mm^2. The new structure of the cylinder is shown in Figure 11.

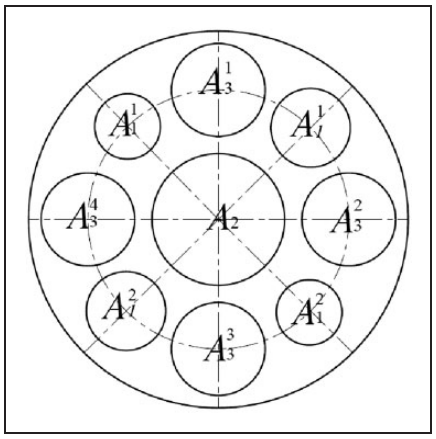

Figure 12. Optimization structure of the multi chambers.

Structural optimization of the multi chambers

To improve the life of the cylinder, it is necessary to optimize the structure of the multi chambers for avoiding the deflection of the main piston. Because the reason leading to the deflection of the main piston is that the composition of the action forces of the plunger rods does not pass the center of the main piston; the solution is to make sure the action force of every plunger rod pass the center of the main piston. In order to achieve the purpose, one plunger chamber is divided into two or more same chambers, and then the same chambers are distributed symmetrically in the circumferential direction. As shown in Figure 12, the chamber A_1 is divided into two same chambers A_1^1 andA_1^2, the chamber A_l is divided into two same chambers A_l^1 andA_l^2 and the chamber A_3 is divided into four same chambers A_3^1, A_3^2, A_3^3 and A_3^4. The chamber A_2 is not divided but whose position is adjusted to be concentric with the main piston. Where the diameter of the chamber A_1^1 orA_1^2 is 5.2 mm, the diameter of the chamber A_l^1 orA_l^2 is 6.3 mm and the diameter of the chamber A_3^1 is 7.4 mm.

In addition, the divided same chambers are only controlled by a switch valve, so oil pressures in them are equal, and then the action forces of the plunger rods in the same chambers are also equal. Because the same chambers are distributed symmetrically in the circumferential direction, the composition of the action forces of the plunger rods pass the center of the

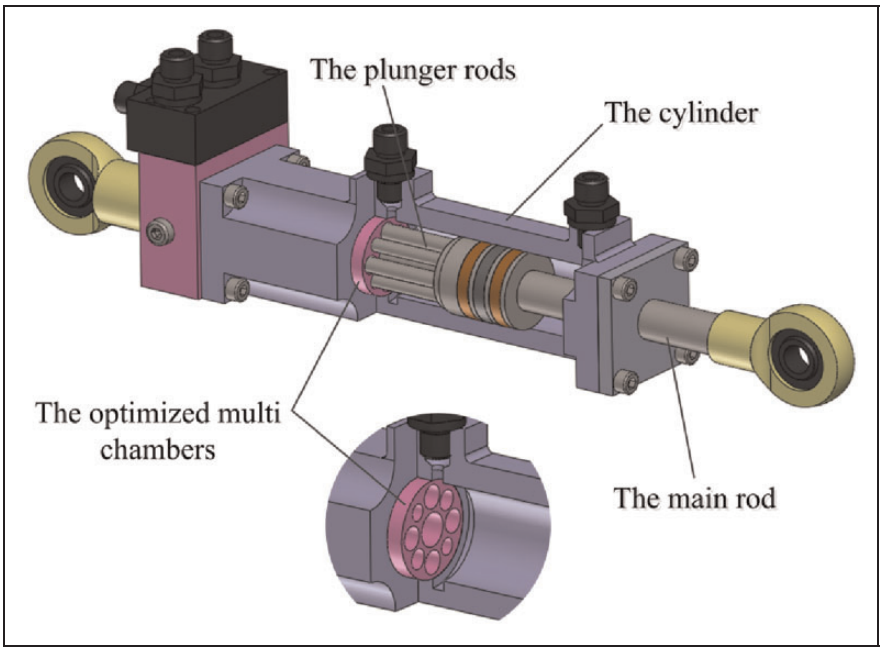

Figure 13. The optimized structure of the new cylinder.

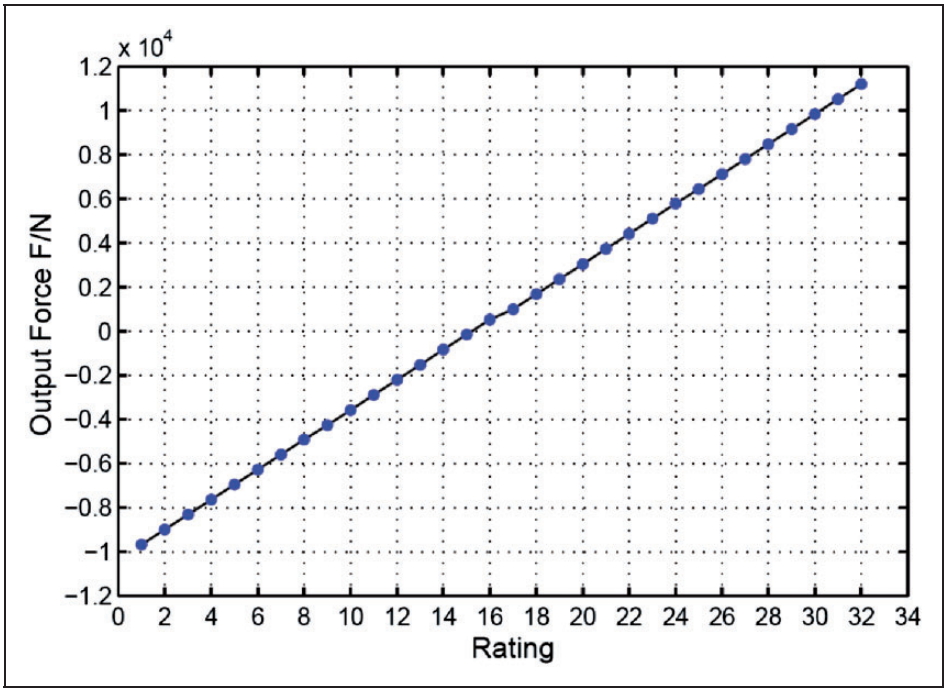

Figure 14. The output force of the optimized cylinder at the different rating.

main piston, so the main piston does not occur to the deflection.

The structure and performance of the optimized cylinder

Based on the optimization design in "Optimization design of the new cylinder" section, the structure of the optimized cylinder is shown in Figure 13. Of course, compared to the original cylinder, the number of the plunger rods of the optimized cylinder is added and the structure of the multi chambers is more complex, but the optimized structure avoids the deflections of the main piston which were caused by the plunger rods' forces, and the optimized cylinder has higher efficiency due to the optimized structure avoids the leakage caused by the deflection of the main piston.

In addition, the output force of the optimized cylinder has been shown in Figure 14. As shown in Figure 14, the output force of the optimized cylinder does not have the jump which appears in Figure 5. Therefore, due to the adjusting range of the output force between a rating and an adjacent rating is almost equal, the optimized cylinder has the better performance of the load matching versus the original cylinder.

Discussion and conclusion

In this paper, a new kind of cylinder with variable effective area was proposed. The principle of varying effective area and the structure of the cylinder was presented. Mathematic models were built to evaluate the performances of the new cylinder. The analyzed results showed that the output force of the new cylinder had a jump and the deflections of the main piston would cause the inner leak of the cylinder. Then the structure of the cylinder was optimized. The optimized cylinder avoided the deflection and had well performance of the load match.

Recently, the hydraulic systems of most power autonomous robots are formed through multiple classical valve-controlled cylinders which have a generally rapid response.[1–5] But the efficiency of the hydraulic system is lowered by producing a lot of throttling losses as the cylinder has widely fluctuating load forces; but the effective area of the cylinder is invariable. This paper shows that the new cylinder can adjust the effective area with the change of the load force and allow energy recovery to reduce throttling losses. Meanwhile, the new cylinder also has a generally rapid response through reserving the classical valve-control. The high efficiency has great significance for power autonomous robots.

In future research, the switching valves will be studied to integrate with the cylinder in order to shorten the lengths of oil circuits and reduce the unnecessary weights. The dimension of the switching valve is the key factors. Under satisfying the flow rate, the dimension is demanded as small as possible. Of course, the Lee valve is a good choice for its small dimension relative to existing products, but it is generally expensive. Considering that the low switching valve frequency is enough, the switching valves driven by small motors will also be studied in the next study.

Declaration of Conflicting Interests

The author(s) declared no potential conflicts of interest with respect to the research, authorship, and/or publication of this article.

Funding

The author(s) disclosed receipt of the following financial support for the research, authorship, and/or publication of this article: This work is supported by the National Natural Science Foundation of China (No. 51205400).

References

1. Amundson K, Raade J, Harding N, et al. Development of hybrid hydraulic-electric power units for field and service robots. *Adv Rob* 2006; 20(9): 1015–1034.
2. Raibert M, Blankespoor K, Nelson G, et al. Bigdog, the rough-terrain quadruped robot. In: *Proceedings of the 17th IFAC world congress*, 2008. Seoul, Korea. pp.10822–10825.
3. Raibert M. Dynamic legged robots for rough terrain. In: *Proceedings of the 10th IEEE-RAS international conference on humanoid robots*, 2010. Nashville, TN, USA.
4. Bhatti J and Plummer AR. Hydraulic running robots: the prospects for fluid power in agile locomotion. In: *Proceedings of the twelfth Scandinavian international conference on fluid power*, 2011. Tampere, Finland.
5. McGee TG, Raade JW and Kazerooni H. Monopropellant-driven free piston hydraulic pump for mobile robotic systems. *J Dyn Syst Meas Control* 2004; 126: 75–81.
6. Durfee W, Xia J and Hsiao-Wecksler E. Tiny hydraulics for powered orthotics. In: *Proceeding of the 2011 IEEE international conference on rehabilitation robotics*, 2011. Rehab Week Zurich, ETH Zurich Science City, Switzerland, pp.978–984.
7. David H and Michael F. Energy-efficient actuation. *Des News* 2013; 8: 40–45.
8. Raade JW, Amundson KR and Kazerooni H. Development of hydraulic-electric power unit for mobile robots. *ASME Int Mech Eng Congr Expos* 2005; 11: 1–8.
9. Semini C, Tsagarakis NG, Guglielmino E, et al. Design of HyQ – a hydraulically and electrically actuated quadruped robot. *Proc IMechE, Part I: J Systems and Control Engineering* 2011; 225: 831–849.
10. Bhounsule P, Cortell J and Ruina A. Design and control of ranger: an energy-efficient, dynamic walking robot. In: *CLAWAR 2012 – proceedings of the fifteenth international conference on climbing and walking robots and the support technologies for mobile machines*, 2012. Vol. 23, pp.441–448.
11. Seok S, Wang A, Chuah MY, et al. Design principles for highly efficient quadrupeds and implementation on the MIT Cheetah robot. In: *Proceedings of the 2013 IEEE international conference on robotics and automation (ICRA)*, 2013. Karlsruhe, Germany, pp.3307–3312.
12. Ruina A. (2012, September) Cornell ranger 2011, 4-legged bipedal robot. http://ruina.tam.cornell.edu/research/topics/locomotion_and_robotics/ranger/Ranger2011
13. Zoss AB, Kazerooni H and Chu A. Biomechanical design of the berkeley lower extremity exoskeleton. *IEEE/ASME Trans Mechatron* 2006; 11: 128–138.
14. Guglielmino E, Kogler H, Semini C, et al. Energy efficient fluid power in autonomous legged robotics. In: *Proceedings of the ASME 2009 dynamic systems and control conference*, 2009. Hollywood, CA, USA, pp.1–8.
15. Guglielmino E, Semini C, Kogler H, et al. Power hydraulics-switched mode control of hydraulic actuation. In: *Proceedings of the 2010 IEEE/RSJ international conference on intelligent robots and systems*, 2010. Taipei, Taiwan. pp.3031–3036.
16. Pan M, Johnston N and Hillis A. Active control of pressure pulsation in a switched inertance hydraulic system. *Proc IMechE, Part I: J Systems and Control Engineering* 2013; 227: 610–620.
17. Alfayad S, Ouezdo FB, Namoun F, et al. Lightweight high performance integrated actuator for humanoid robotic applications: modeling, design & realization. In: *IEEE international conference on robotics and automation*, 2009. Kobe, Japan, pp.562–567.
18. Zimmerman J and Ivantysynova M. Hybrid displacement controlled multi actuator hydraulic systems. In: *The twelfth Scandinavian international conference on fluid power*, SICFP11, 2011. Tampere, Finland.
19. Williamson C, Zimmerman J and Ivantysynova M. efficiency study of an excavator hydraulic system based on displacement-controlled actuators. In: *Bath/ASME symposium on fluid power and motion control (FPMC 2008)*, 2008. Bath, UK.
20. Tuokko RO. Analysis of alternative oil flow control methods for high-power hydraulic servocylinders. *Proc IMechE, Part A: J Power and Energy* 1990; 204: 163.
21. Payne G, Kiprakis A, Eshan M, et al. Efficiency and dynamic performance of digital displacement TM hydraulic transmission in tidal current energy converters. *Proc IMechE, Part A: J Power and Energy* 2007; 221: 207–218.
22. Shen W, Jiang J, Su X, et al. A new type of hydraulic cylinder system controlled by the new-type hydraulic transformer. *Proc IMechE, Part C: J Mechanical Engineering Science* 2014; 228: 2233.
23. Yoon JI, Kwan AK and Truong DQ. A study on an energy saving electro-hydraulic excavator. In: *Proceedings of the ICROS-SICE international joint conference*, 2009. Fukuoka, Japan. pp.3825–3830.
24. Seung C and Petr N. Position tracking control with load-sensing for energy-saving valve-controlled cylinder system. *J Mech Sci Technol* 2012; 26: 617–625.
25. Shenouda A. Quasi-static hydraulic control systems and energy savings potential using independent metering four-valve assembly configuration. Woodruff School of Mechanical Engineering, Georgia Institute of Technology, 2006.
26. Eriksson B and Palmberg J-O. Individual metering fluid power systems: challenges and opportunities. *Proc IMechE, Part I: J Systems and Control Engineering* 2011; 225: 196–211.
27. Summers-Smith JD. *Mechanical seal practice for improved performance*, 2nd ed. London: Mechanical Engineering Publication Ltd, 1992.

Appendix

Notations

A_{sw}	opening area of switching valve
C_d	coefficient of flow for servo valve
C_{sw}	coefficient of flow for switching valve
D	diameter of main Rod
D	diameter of main Piston
E	material elastic modulus
I	inertia moment of the main rod
L	length of the main piston
L	stroke of the cylinder
P_o	pressure of tank
P_s	pressure of power source
R	diameter of the main piston
R_1	distance from the point O to K_1
R_2	distance from the point O to K_2
R_3	distance from the point O to K_3
R_4	distance from the point O to K_l
U	opening of servo valve
U	velocity of piston rod
V	velocity of piston rod
W	spool circumference of servo valve
x_k	on–off value of four switching valves
ρ	density of oil
α	acute angle between the y axis and the beeline OK_1
β	acute angle between the y axis and the beeline OK_2
γ	acute angle between the y axis and the beeline OK_3
δ	gap between piston and inner wall
μ	dynamic viscosity
ε	relative precision